

Magnetization and specific heat of LaTiO₃

V. Fritsch,¹ J. Hemberger,¹ M. V. Eremin,^{1,2} H.-A. Krug von Nidda,¹ F. Lichtenberg,³ R. Wehn,¹ and A. Loidl¹

¹*Experimentalphysik V, EKM, Institut für Physik, Universität Augsburg, 86135 Augsburg, Germany*

²*Kazan State University, 420008 Kazan, Russia*

³*Experimentalphysik VI, EKM, Institut für Physik, Universität Augsburg, 86135 Augsburg, Germany*

(Received 20 March 2002; published 20 May 2002)

The orbital ground state of LaTiO₃ is still under debate. Recent letters [Phys. Rev. Lett. **85**, 3950 (2000); **85**, 3946 (2000)] discussed a scenario of an orbital liquid, and provided theoretical predictions about orbital contributions to the specific heat. Here we present the results of heat capacity and magnetic measurements. Based on model calculations we determine an electronic ground state which gives g values compatible with the experimentally observed ordered moment and the paramagnetic susceptibility. The heat capacity of LaTiO₃ is compared with that of orbitally ordered LaMnO₃. We conclude that most of the low-temperature heat capacity arises from magnon contributions in both LaMnO₃ and LaTiO₃.

DOI: 10.1103/PhysRevB.65.212405

PACS number(s): 75.30.Cr, 75.30.Et, 71.27.+a, 71.30.+h

Orbital degrees of freedom, in addition to spin, charge, and lattice structure, are gaining increasing interest in current solid-state physics. That is, in manganites the question of orbital order plays a key role in the understanding of electronic properties such as the colossal magnetoresistant effect¹ or the existence of ferromagnetic insulating ground states.^{2,3} Orbital order has been experimentally verified for several compounds. Finally the experimental observation of orbitons in LaMnO₃ as elementary collective excitations within the orbitally ordered state has been reported.⁴

LaTiO₃ is an antiferromagnetic $3d^1$ Mott-Hubbard insulator with a Néel temperature of $T_N = 146$ K. It can roughly be characterized as a pseudocubic perovskite, with degenerate t_{2g} orbitals. The role of the orbital degrees of freedom in this system is still unclear. Recently Khaliullin and Maekawa⁵ proposed a theory to explain the anomalies of the neutron-scattering and x-ray results observed by Keimer *et al.*⁶ According to the Goodenough-Kanamori rules one expects local ferrotypic orbital correlations in a spin Néel state, but no evidence of orbital order in LaTiO₃ was found.⁶ Treating the problem within mean-field (MF) theory, Khaliullin and Maekawa found a finite MF order parameter, which evokes an orbital gap. They also predicted that a linear term in the specific heat should be released when the correlation gap in the orbital spectrum becomes thermally washed out.⁵ Because of the small distortion of the TiO₆ octahedra in LaTiO₃ the crystal field acting on the Ti³⁺ ions (Ti³⁺: $3d^1$) is nearly cubic.⁶ Hence there is a threefold-degenerate t_{2g} band, occupied by one electron in LaTiO₃. From this a disordered orbital liquid ground state is predicted, where the orbital degrees of freedom are interacting via magnons and which is dominated by fluctuations.⁵ In the orthorhombic perovskite LaMnO₃ (Mn³⁺: $3d^4$) one finds a different scenario. Here the e_g band is occupied by one electron, the degeneracy is lifted by the Jahn-Teller (JT) effect, and the orbitals are ordered. The purpose of this work is to give a detailed characterization of the electronic and thermodynamic properties of LaTiO₃, and to relate these to a possible orbital origin in comparison to LaMnO₃.

Single crystals of LaTiO₃ have been prepared by the floating zone melting as described elsewhere.⁷ The oxygen con-

tent was determined thermogravimetrically. The x-ray-diffraction pattern at room temperature reveals an orthorhombic structure with the lattice parameters $a = 5.633$ Å, $b = 5.617$ Å, and $c = 7.915$ Å. These lattice parameters are almost cubic and close to those reported in the literature (e.g., Ref. 8). The slight distortion from cubic symmetry results from a buckling of the oxygen octahedra. Note that for LaTiO₃ we find $a \sim b > c/\sqrt{2}$, characteristic of the O'-type structure, indicative of an additional JT distortion superimposed on the O-orthorhombic structure which results from geometrical constraints only. For comparison we show heat-capacity results on single crystalline LaMnO₃ ($T_N = 140$ K and $T_{JT} = 800$ K) which also shows the O' structure, though with a much stronger JT distortion. For further details the reader is referred to Ref. 3.

The magnetization measurements were performed with a commercial superconducting quantum interference device system between 1.8 and 400 K, and in magnetic fields up to 50 kOe. Additional measurements were done, employing an extraction magnetometer for higher fields and an ac susceptibility. No geometric demagnetization effects had to be considered due to the small absolute value of the ferromagnetic magnetization (see below). The specific heat has been measured with noncommercial setups utilizing a quasi-adiabatic method between 2 and 15 K, and an ac method between 10 and 300 K.

It is known that LaTiO₃ is sensitive to deviations from its nominal stoichiometry.^{7,9-11} Stoichiometric LaTiO₃ is known as a canted antiferromagnet, with a G -type structure and a small canting angle. The ordered antiferromagnetic moment is of the order of $0.45\mu_B$,^{7,8,12} while the ferromagnetic moment in the stoichiometric compound amounts to $0.015\mu_B$. The weak ferromagnetism arises from the antisymmetric Dzyaloshinski-Moriya exchange, which becomes allowed via the buckling of the oxygen octahedra. The inset of Fig. 1 displays the ac susceptibility of the sample investigated in this paper in the vicinity of the transition into a canted antiferromagnetic state. The sharp peak in the real part determines the magnetic transition temperature at $T_N = 146$ K, corresponding to the highest transition temperatures reported in the literature.^{7,8} Already small deviations in stoichiometry

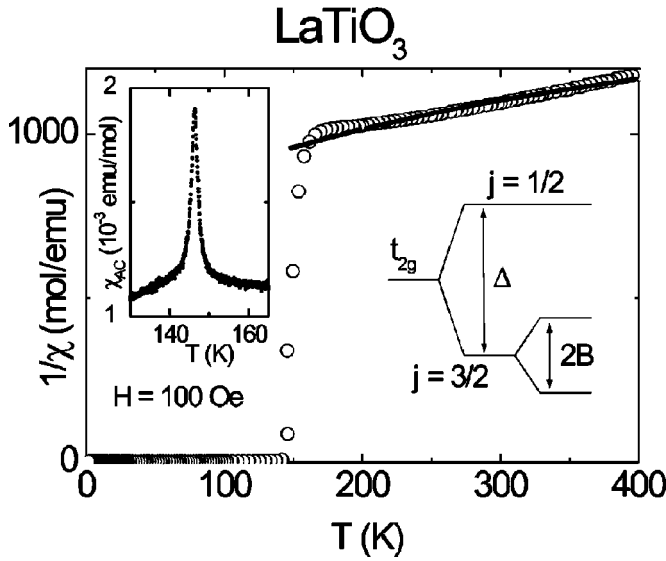


FIG. 1. Inverse dc susceptibility $1/\chi$ of LaTiO_3 in an external field of 100 Oe. The sketched scheme of energy levels denotes the expected single-ion electronic configuration in the paramagnetic phase for LaTiO_3 . The solid line is calculated as described in text. Inset: ac susceptibility of LaTiO_3 in a stimulating magnetic field of 0.2 Oe_{rms} measured at a frequency of 3333 Hz.

lower the Néel temperature T_N dramatically. The electric resistivity (not displayed) reveals an insulating behavior at all temperatures with a value of 1 k Ω cm at T_N . According to the literature,^{7,9,13} the Mott-Hubbard-insulator LaTiO_3 is driven toward a metallic state on oxygen surplus or a lanthanum deficiency, and thus the high resistivity of our sample compared to published data indicates the absence of any deviations from the nominal composition.

Figure 1 displays the inverse dc susceptibility $1/\chi$ measured at a field of $H=100$ Oe. Below T_N the signal is dominated by the rise of a weak spontaneous ferromagnetic component, while above $1/\chi$ shows a nearly linear increase toward higher temperatures. The small but distinct slope of this curve for temperatures up to 400 K indicates that the paramagnetic susceptibility can be described neither by a Curie-Weiss-type behavior nor by a constant Pauli contribution. Indeed, the latter is not expected due to the insulating character of the conductivity, above as well as below T_N . If one tries to parametrize χ^{-1} in terms of a Curie-Weiss law, one ends up with an effective moment of $3.2\mu_B$ and a Curie-Weiss temperature of -1100 K, both values beyond any physical interpretation.

The distortion of the TiO_6 octahedra in LaTiO_3 is rather small, and therefore one should take the spin-orbit coupling into account. Considering spin-orbit coupling and the local axial crystal field,^{14,15} one arrives at the energy-level scheme for Ti^{3+} sketched in Fig. 1. The susceptibility is dominated by a Van Vleck contribution, with an expected spin-orbit splitting value $\Delta=330$ K.^{16,17} The effective g value for the pure quadruplet $j=3/2$ is zero, but becomes sizable and anisotropic due to j mixing caused by the axial crystal field. The solid line in Fig. 1 is fitted superposing the susceptibility contributions of the four inequivalent Ti places and using the

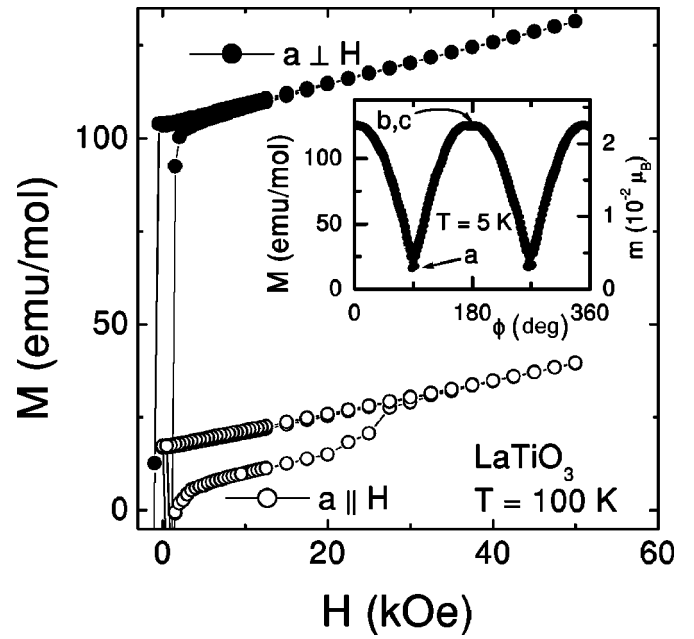


FIG. 2. Hysteresis loops of LaTiO_3 with different angles ϕ between the b,c plane and the magnetic field at a temperature $T=100$ K in magnetic fields up to 50 kOe. Inset: magnetization of LaTiO_3 at a temperature $T=5$ K in dependence on the angle ϕ between the b,c plane and the magnetic field.

spin-orbit value $\Delta=330$ K and an exchange-coupling parameter $J=85$ K.¹⁷ This yields a crystal-field parameter $B=26$ K from which the g values can be calculated, resulting in $g_{\parallel}=0.7$ and $g_{\perp}=0.35$ in accordance with the estimates of Ref. 6. This corresponds to an effective paramagnetic moment $\mu_{eff}=\sqrt{j(j+1)}g\mu_B=0.9\mu_B$ using the average $g=\frac{1}{3}g_{\parallel}+\frac{2}{3}g_{\perp}=0.46$. It should be mentioned that angle-dependent measurements of the susceptibility in the paramagnetic regime ($T=300$ K, not shown) reveal an anisotropy of about 10%. This is smaller than the value of 25% expected on the basis of this model, which is described in detail elsewhere.¹⁷ The experimental data of $1/\chi$ curve up slightly, while the fit has a downward curvature. This inconsistency may be explained by short-range correlations near the magnetic phase transition.

In the magnetically ordered regime a significant anisotropy arises. The inset of Fig. 2 shows an angle-dependent measurement of the magnetization in LaTiO_3 at $T\approx 100$ K on a single crystal, which was confirmed to be untwinned via Laue pictures. However, a slight misorientation cannot be ruled out. The angle ϕ characterizes the position of the a axis with respect to the external field of $H=20$ kOe. The minima of $M(\phi)$ correspond to the field lying parallel to the a axis, whereas for the maxima the field is applied within the b,c plane. The angular dependence of $M(\phi)$ can be described using a $\cos \phi$ term and a constant offset. The easy axis of the ferromagnetic component lies in the b,c plane. Under rotation only the projection of the spontaneous magnetization onto the field direction is measured. When the ferromagnetic component in the b,c plane is perpendicular to the external field H , it will be flipped under further rotation, so that its projection always points in the direction of H .

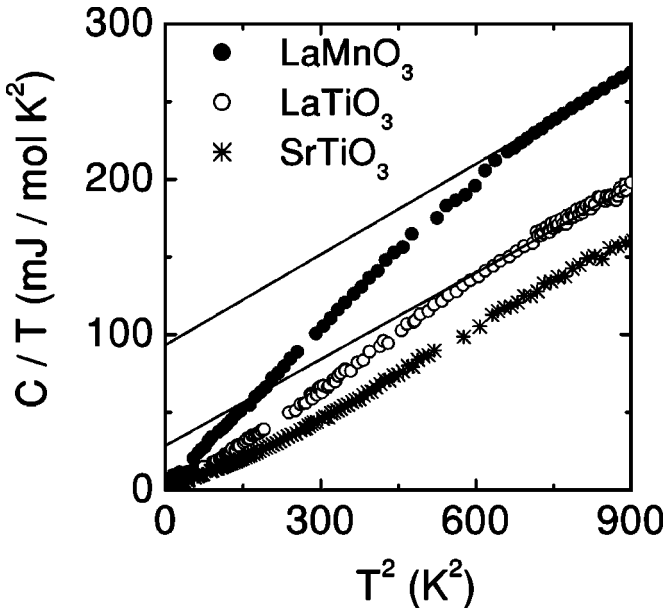


FIG. 3. Specific heat of LaTiO_3 (open circles \circ), SrTiO_3 (stars $*$), and LaMnO_3 (closed circles \bullet) plotted on a quadratic temperature scale. The solid lines are extrapolated from the linear part $\propto \gamma T$ of the specific heat at temperatures between 15 and 25 K.

The hysteresis loops shown in Fig. 2 are taken at $T = 100$ K along the a direction (\circ) and in the b, c plane (\bullet), respectively. The coercivity and the small remnance along the a axis may also result from the above-mentioned uncertainty in the orientation. The remnance and coercive field measured in the b, c plane establish a distinct spontaneous magnetization which vanishes for the a direction. On increasing external fields, the magnetization increases linearly up to 10 T (not shown). The spontaneous contribution to the magnetization can be explained by Dzyaloshinsky-Moriya (DM) interactions.¹⁸ A similar behavior is known, e.g., from manganites.^{3,19} By minimizing the free energy consisting of isotropic superexchange, antisymmetric (DM) exchange, easy-axis anisotropy, and Zeeman energy, the magnetic moment composed of the spontaneous ferromagnetic and the induced magnetic moment was calculated.¹⁷ While the spontaneous ferromagnetic moment is equal to the remnant magnetization of the hysteresis loop perpendicular to the a axis, the induced magnetic moment can be evaluated from the slope of this loop. This leads to a canting angle θ of nearly 3° and to a g value of 0.25, resembling an ordered moment $\mu_{ord} = g\mu_B j_z = 0.5\mu_B$, which both fits within the error bars to the result of Meijer *et al.*⁸ From the canting angle one can determine the strength D of the DM interaction via $D/J = \tan(2\theta)$. One finds $D = 4.5$ K, which is of the same order of magnitude as the result obtained from magnon dispersion by Keimer *et al.*⁶

To study a possible contribution from the orbital liquid ground state in LaTiO_3 , we focused on lower temperatures, where it is easier to take into account phonon contributions and where distinct theoretical predictions have been made.⁶ Figure 3 shows the specific heat of LaTiO_3 , LaMnO_3 , and SrTiO_3 (Ref. 20) plotted as C/T versus T^2 . This representation displays phononic contributions ($\propto T^3$) to the specific

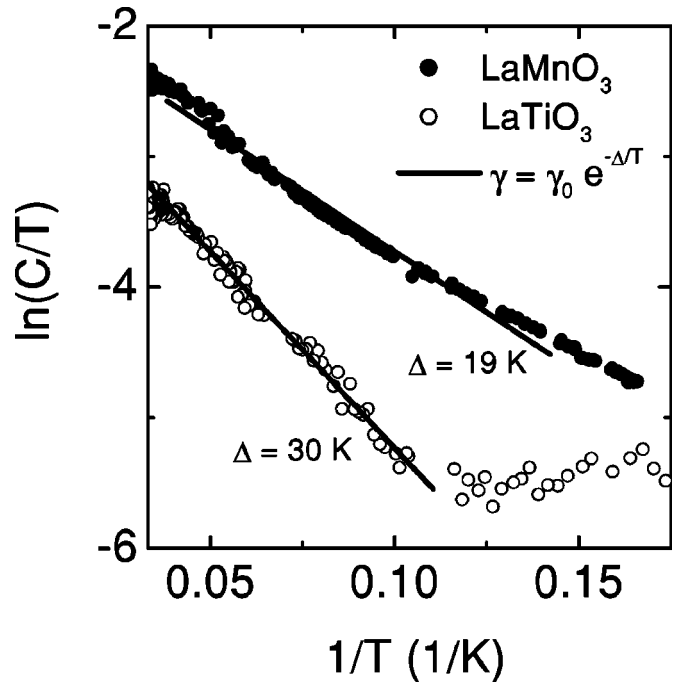


FIG. 4. Magnetic contribution to the specific heat of LaMnO_3 (closed circles \bullet) and LaTiO_3 (open circles \circ), where the specific heat of SrTiO_3 is subtracted, as $\ln(C/T)$ vs $1/T$. The solid lines are linear fits assuming $\gamma = \text{const} + \gamma_0 e^{-\Delta/T}$.

heat as a linear increase. Linear contributions (γT) appear as the extrapolated value for $T=0$. All compounds are insulators, and hence a Sommerfeld coefficient $\gamma_s = 0$ is expected. However, as mentioned above, a similar “quasiparticle” contribution was postulated for an orbital liquid.⁵ C/T vs T^2 in SrTiO_3 shows a nearly linear behavior due to phonons. The solid lines in Fig. 3 are extrapolations of the linear part of the specific heat in LaTiO_3 and LaMnO_3 at temperatures between 15 and 30 K. The deviations from this linear behavior indicate the presence of a gap in the “quasiparticle” density of states in LaTiO_3 and in LaMnO_3 . Toward lower temperatures these finite γ contributions become suppressed. For LaTiO_3 this contribution can be estimated to be $\gamma \approx 31$ mJ/mol K^2 , in good agreement with the value of 40 mJ/mol K^2 estimated by Khaliullin and Maekawa for an orbital liquid ground state.⁵ Due to the existing orbital order for LaMnO_3 such a contribution is not expected but the experimentally observed γ value is even larger (Fig. 3).

To estimate the underlying gap energies, we tried to subtract the lattice part of the specific heat in the low-temperature regime. For that purpose we used SrTiO_3 as a reference material, as it possesses neither magnetic nor orbital degrees of freedom. Nevertheless, it has to be noted that, in most perovskites, an excess contribution from low-lying optical phonons has to be considered, even for temperatures below 50 K.²¹ These soft-mode effects are strongest in SrTiO_3 because of its incipient ferroelectricity, and explain the small nonlinearities in Fig. 3. Comparing these with the nonlinear features of LaMnO_3 and LaTiO_3 again makes clear that the latter have a different origin. Subtracting the data of SrTiO_3 should eliminate all phonon contributions (or at the

worst overdo a little). For temperatures below 12 K, Woodfield *et al.*²² examined the specific heat of LaMnO₃. They found a vanishing linear contribution γ_s in accordance to our results, and showed the importance of hyperfine contributions for temperatures below $T \approx 5$ K. Such types of contributions are not present, or else they differ in SrTiO₃ or LaTiO₃. Thus for this lowest temperature the subtraction of the SrTiO₃ data cannot separate magnetic or orbital contributions. For this we restricted our analysis to the temperature range $30 > T > 5$ K. The results for ΔC_p are shown in Fig. 4. We assume that the opening of the gap in a restricted temperature regime $T \approx \Delta$ yields $\gamma = \gamma_0 e^{-\Delta/T}$. Plotting the logarithm of ΔC_p versus $1/T$ demonstrates that such a type of behavior can indeed be detected, and the representation of Fig. 4 shows a linear regime between 10 and 25 K. We are aware that the exponential behavior extends only over a limited temperature range below the gap. As mentioned above, additional nuclear contributions lead to deviations toward lower temperatures. In the case of LaTiO₃ a very small additional linear contribution to the specific heat seems to exist. Thus the determined gap values have to be considered as rough estimations only. For LaTiO₃ one finds $\Delta \approx 30$ K, equivalent to 2.6 meV. This value is close to the magnon gap $\Delta = 3 \pm 0.3$ meV found by Keimer *et al.* by neutron

scattering.⁶ For LaMnO₃ we determined an energy gap of $\Delta = 1.7$ meV. Mitsudo *et al.*²³ reported a magnon gap of 2.1 meV for LaMnO₃. The good agreement of the heat-capacity results with neutron-scattering data for both antiferromagnetic compounds implies that the additional specific-heat contribution has to be attributed to magnons rather than to orbital degrees of freedom. From this point of view it seems that in LaTiO₃ the orbital degrees of freedom are also quenched.

In conclusion, we presented measurements of the magnetization and the specific heat of LaTiO₃. The anisotropic magnetization can be explained by small DM interactions. The Van Vleck-type behavior of the susceptibility and the small g factor can be perfectly well explained by means of spin-orbit splitting and small crystal fields. The additional contributions to the specific heat of LaTiO₃ and of orbitally ordered LaMnO₃ can be related to the magnon gaps of these compounds. To clarify the nature of the spin-orbital ground state in LaTiO₃, further investigations are badly needed.

This work was sponsored by the BMBF via VDI/EKM, FKZ 13N6917/18, and by DFG within SFB 484 (Augsburg) and Project No. 436RUS113/628/0. M.V.E. was partially supported by Grant No. RFFI 00-02-17597 and BRHE Program Grant No. REC-007.

-
- ¹E. Dagotto, T. Hotta, and A. Moreo, *Phys. Rep.* **344**, 1 (2001).
²D.I. Khomskii, *Int. J. Mod. Phys. B* **15**, 2665 (2001).
³M. Paraskevopoulos, F. Mayr, C. Hartinger, A. Pimenov, J. Hemberger, P. Lunkenheimer, A. Loidl, A.A. Mukhin, V.Yu. Ivanov, and A.M. Balbashov, *J. Magn. Magn. Mater.* **211**, 118 (2000).
⁴E. Saitoh, S. Okamoto, K.T. Takahashi, K. Tobe, K. Yamamoto, T. Kimura, S. Ishihara, S. Maekawa, and Y. Tokura, *Nature (London)* **410**, 180 (2001).
⁵G. Khaliullin and S. Maekawa, *Phys. Rev. Lett.* **85**, 3950 (2000).
⁶B. Keimer, D. Casa, A. Ivanov, J.W. Lynn, M.v. Zimmermann, J.P. Hill, D. Gibbs, Y. Taguchi, and Y. Tokura, *Phys. Rev. Lett.* **85**, 3946 (2000).
⁷F. Lichtenberg, D. Widmer, J.G. Bednorz, T. Williams, and A. Reller, *Z. Phys. B: Condens. Matter* **82**, 211 (1991); F. Lichtenberg, A. Herrmberger, K. Wiedenmann, and J. Mannhart, *Prog. Solid State Chem.* **29**, 1 (2001).
⁸G.I. Meijer, W. Henggeler, J. Brown, O.-S. Becker, J.G. Bednorz, C. Rossel, and P. Wachter, *Phys. Rev. B* **59**, 11 832 (1999).
⁹V. Fritsch, J. Hemberger, M. Brando, A. Engelmayer, S. Horn, M. Klemm, G. Knebel, F. Lichtenberg, P. Mandal, F. Mayr, M. Nicklas, and A. Loidl, *Phys. Rev. B* **64**, 045113 (2001).
¹⁰Y. Okada, T. Arima, Y. Tokura, C. Murayama, and N. Môri, *Phys. Rev. B* **48**, 9677 (1993).
¹¹Y. Taguchi, T. Okuda, M. Ohashi, C. Maurayama, N. Môri, Y. Iye, and Y. Tokura, *Phys. Rev. B* **59**, 7917 (1999).
¹²J.P. Goral and J.E. Greedan, *J. Magn. Magn. Mater.* **37**, 315 (1983).
¹³D.A. Crandles, T. Timusk, J.D. Garrett, and J.E. Greedan, *Phys. Rev. B* **49**, 16 207 (1994).
¹⁴M. Eitel and J.E. Greedan, *J. Less-Common Met.* **116**, 95 (1986).
¹⁵*International Table for Crystallography, Vol. A: Space Group Symmetry*, edited by T. Hahn (Kluwer, Dordrecht, 1996).
¹⁶A. Abragam and B. Bleaney, *Electron Paramagnetic Resonance* (Clarendon Press, Oxford, 1970).
¹⁷M. V. Eremin (unpublished).
¹⁸F. Keffer, *Phys. Rev.* **126**, 896 (1962).
¹⁹A. Pimenov, M. Biberacher, D. Ivannikov, A. Loidl, V.Y. Ivanov, A.A. Mukhin, and A.M. Balbashov, *Phys. Rev. B* **62**, 5685 (2000).
²⁰J. Hemberger, M. Nicklas, P. Lunkenheimer, A. Loidl, and R. Böhmer, *J. Phys.: Condens. Matter* **8**, 4673 (1996).
²¹W. Lawless and W. Morrow, *Ferroelectrics* **15**, 159 (1977).
²²B.F. Woodfield, M.L. Wilson, and J.M. Byers, *Phys. Rev. Lett.* **78**, 3201 (1997).
²³S. Mitsudo, K. Hiran, H. Nojira, M. Motokawa, K. Hirota, A. Nishizawa, N. Kaneko, and Y. Endoh, *J. Magn. Magn. Mater.* **177-181**, 877 (1998).